JOC Article

Matrix Isolation and EPR Spectroscopy of Septet 3,5-Difluoropyridyl-2,4,6-trinitrene

Sergei V. Chapyshev,*,† Dirk Grote,‡ Christopher Finke,‡ and Wolfram Sander*,‡

Lehrstuhl für Organische Chemie II, Ruhr-Universität, D-44780 Bochum, Germany, and Institute of Problems of Chemical Physics, Russian Academy of Sciences, 142432 Chernogolovka, Moscow Region, Russia

chap@icp.ac.ru; wolfram.sander@rub.de

Received February 26, 2008

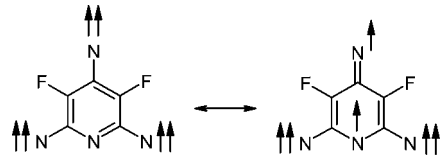

Septet Trinitrene

Septet 3,5-difluoropyridyl-2,4,6-trinitrene along with quintet 2-azido-3,5-difluoropyridyl-4,6-dinitrene, quintet 4-azido-3,5-difluoropyridyl-2,6-dinitrene, triplet 2,6-diazido-3,5-difluoropyridyl-4-nitrene, and triplet 2,4-diazido-3,5-difluoropyridyl-6-nitrene have been obtained by photolysis of 2,4,6-triazido-3,5-difluoropyridine in solid argon at 4 K. The electronic and magnetic properties of the matrix-isolated nitrenes were studied using electron paramagnetic resonance (EPR) spectroscopy in combination with density functional theory (DFT) calculations. The fine-structure parameters of the nitrenes were determined with high accuracy from computer spectral simulations. All signals in the EPR spectra of the nitrenes randomly oriented in the solid phase were unambiguously assigned on the basis of eigenfield calculations of the Zeeman energy levels and angular dependencies of resonance fields from the direction of the applied magnetic field.

Introduction

Among all organic hexaradicals, septet trinitrenes have the largest zero-field splitting (zfs) *D*-parameters and are of considerable interest as model systems for explorations of magnetism in high-spin organic molecules with strong one-center spin−spin interactions and π-robust spin polarization.[1−3] Recently, the first four representatives of such trinitrenes, **1**,[1] **2**,[1] **3**,[2] and **4**,[3] have successfully been obtained in cryogenic matrices and characterized by EPR spectroscopy (Scheme 1).

Because septet trinitrenes have rather high spin populations on the diradical sites and need six additional electrons to complete their electronic shells, they are very electron-deficient and readily react with the surrounding medium or undergo intramolecular rearrangements to form low-spin products. Therefore, attempts to obtain these highly reactive intermediates by low-temperature solid-phase photolysis of the respective triazides quite often were unsuccessful.[4−6] Thus, for instance, our previous attempts to record EPR spectra of septet trinitrene **10** during the photolysis of triazide **5** in organic glasses at 77

SCHEME 1. Septet Trinitrenes Studied Previously

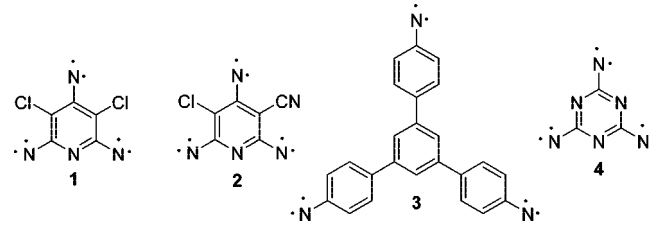

† Russian Academy of Sciences.

‡ Ruhr-Universität Bochum.

(1) Chapyshev, S. V.; Walton, R.; Sanborn, J. A.; Lahti, P. M. *J. Am. Chem. Soc.* **2000**, *122*, 1580–1588.

(2) Oda, N.; Nakai, T.; Sato, K.; Shiomi, D.; Kozaki, M.; Okada, K.; Takui, T. *Synth. Met.* **2001**, *121*, 1840–1841.

(3) Sato, T.; Narazaki, A.; Kawaguchi, Y.; Niino, H.; Bucher, G.; Grote, D.; Wolff, J. J.; Wenk, H. H.; Sander, W. *J. Am. Chem. Soc.* **2004**, *126*, 7846–7852.

(4) Moriarty, R. M.; Rahman, M.; King, G. *J. Am. Chem. Soc.* **1966**, *88*, 842–843.

(5) Wasserman, E.; Schueller, K.; Yager, W. A. *Chem. Phys. Lett.* **1968**, *2*, 259–260.

(6) Nakai, T.; Sato, K.; Shiomi, D.; Takui, T.; Itoh, K.; Kozaki, M.; Okada, K. *Mol. Cryst. Liq. Cryst.* **1999**, *334*, 157–166.

10.1021/jo800425k CCC: $40.75 © 2008 American Chemical Society
Published on Web 08/19/2008

SCHEME 2. Triplet, Quintet, and Septet Nitrenes Formed in the Photolysis of Triazide 5

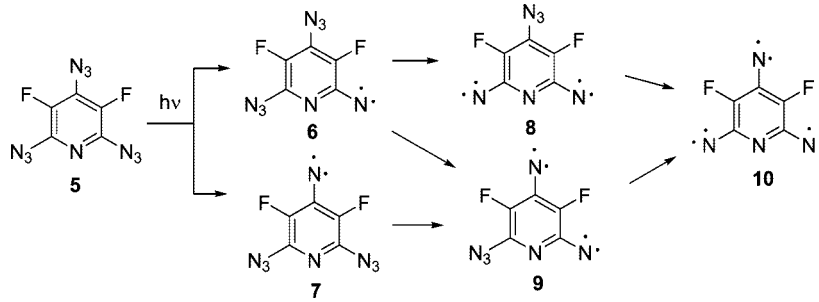

K allowed us only to detect EPR signals of triplet nitrene **7** and quintet dinitrene **9** (Scheme 2).[1]

Similar results have also been obtained during the photolysis of 2,4,6-triazido-1,3,5-triazine in crystals at 4.5 K.[6] As was shown in recent studies, septet trinitrene **4** is formed from this triazide only if the photolysis is carried out in argon matrices at temperatures below 15 K.[3] This finding prompted us to reinvestigate the photolysis of triazide **5** in solid argon at 4 K. Taking into account the high resolution of EPR spectra of high-spin molecules in argon matrices,[3] such a study provided a chance to reliably identify all paramagnetic products of the reaction and to assign their EPR signals.

In this work, we report the synthesis of septet trinitrene **10** in solid argon and a detailed EPR study of quintet and septet nitrenes, including the precise determinations of their zfs parameters, complete assignments of all observed EPR signals, and eigenfield calculations of the Zeeman energy levels.

Results and Discussion

Matrix Photolysis: EPR Measurement. Irradiation ($\lambda > 305$ nm) of triazide **5**, matrix-isolated in argon at 4 K, led at the initial stages of the photolysis to the appearance of two characteristic EPR signals at 7032 and 7294 G, which were assigned to X_2Y_2-transitions of triplet nitrenes **6** and **7**. In addition, a series of weak signals in the region of 100−10000 G were assigned to quintet dinitrenes **8** and **9** and septet trinitrene **10** (Figure 1a). On further irradiation, the intensities of the EPR signals of the triplet nitrenes gradually decreased, reaching minimum intensity after 2 h of photolysis. At the same time, the intensities of the EPR signals of the high-spin nitrenes reached their maximum (Figures 1b, 2). The fact that both triplet nitrenes were formed in nearly equal yields and the high intensities of the X_2Y_2-transitions were preserved on prolonged UV irradiation indicated that the photolysis of triazide **5** is not selective, and the triplet nitrenes are photochemically rather stable toward rearrangement in argon matrices. In contrast, the photolysis of 2,4,6-triazido-3,5-dichloropyridine described previously is selective, and one of the two possible triplet nitrenes is formed preferentially.[1,7] The photochemical stability of **6** and **7** is in line with previous observations that fluorine substituents stabilize triplet pyridyl nitrenes toward rearrangements to azirines.[8] Especially stable are triplet pyridyl nitrenes with two fluorine atoms in the *ortho*-positions to the nitrene centers. The more noticeable decay of the signal at 7032 G during prolonged UV irradiation suggests that this signal, most likely, arises from triplet nitrene **6** with only one fluorine atom in the position *ortho* to the nitrene center.

DFT calculations predict that of the two triplet nitrenes **6** and **7** the former has a lower spin density on the nitrene unit ($\rho_N = 1.6680$ and 1.6965 for **6** and **7**, respectively), and therefore its EPR signal should appear at lower resonance fields, which is in line with the assignment based on the relative photochemi-

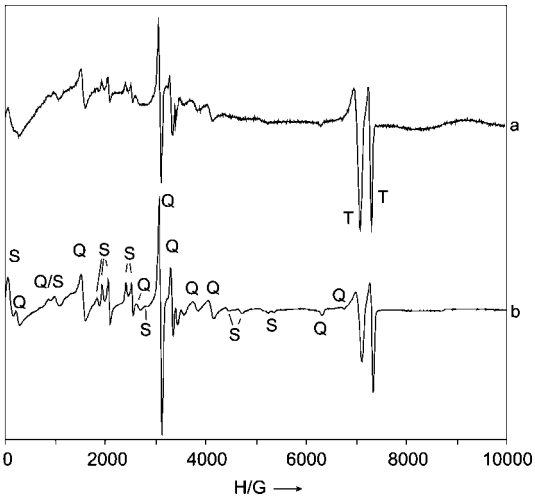

FIGURE 1. EPR spectra: (a) after 5 min; (b) after 2 h of UV irradiation of triazide **5**. The signals are assigned to triplet (T), quintet (Q), and septet (S) species.

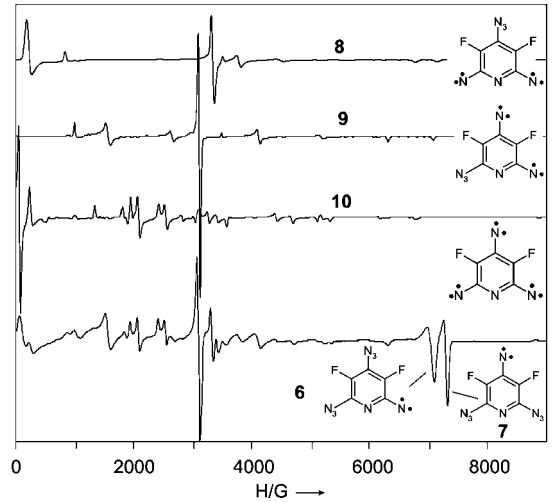

FIGURE 2. Comparison of experimental and simulated EPR spectra: (a) simulated spectrum of dinitrene **8** with $S = 2$, $g = 2.0023$, $D = +0.213$ cm^{-1}, $E = -0.0556$ cm^{-1}; (b) simulated spectrum of dinitrene **9** with $S = 2$, $g = 2.0023$, $D = +0.215$ cm^{-1}, $E = -0.0390$ cm^{-1}; (c) simulated spectrum of trinitrene **10** with $S = 3$, $g = 2.0023$, $D = -0.1018$ cm^{-1}, $E = +0.0037$ cm^{-1}; (d) experimental spectrum (microwave frequency 9.594606 GHz) after 2 h of UV irradiation of triazide **5** in solid argon at 4 K, triplet signals are assigned to nitrene **6** with $S = 1$, $g = 2.0023$, $D = +1.041$ cm^{-1}, $E = 0$ and nitrene **7** with $S = 1$, $g = 2.0023$, $D = +1.143$ cm^{-1}, $E = 0$.

SCHEME 3. Principal Magnetic Axes of Quintet Dinitrenes 8, 9, 11, and 12

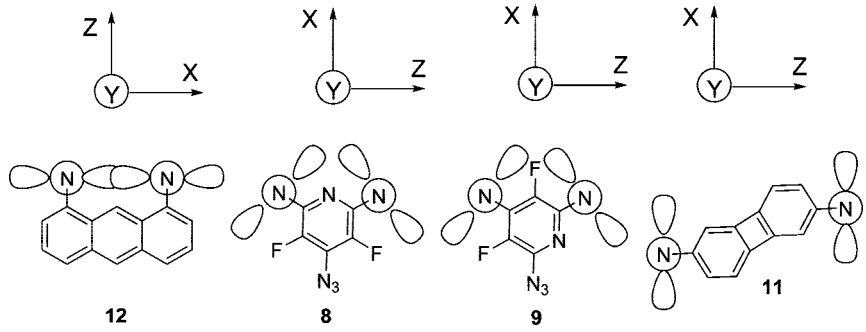

cal stability. The differences in spin densities on the nitrene units of triplet nitrenes **6** and **7** result from different conjugations of these units with the aromatic ring. The nitrene center of **7** lies in the nodal plane of the highest occupied π orbital of pyridine and therefore is less conjugated with the pyridine ring. This results in some lengthening of the C−N bond ($r_{CN} = 1.330$ compared to 1.327 Å for the C−N bond in **6**) and in the higher spin density at the nitrene center as described above.

Extensive studies[9−14] have shown that most aromatic quintet dinitrenes with *meta* orientations of the nitrene units display strong EPR signals of the Y_2-transitions in the region of 2900−3100 G. However, in quintet pyridyl-2,6-dinitrenes these transitions are found at 3200−3400 G.[12−14] This allows the assignment of the two EPR signals at 3305 and 3116 G to Y_2-transitions of the quintet dinitrenes **8** and **9**, respectively. Changes in the intensities of the two EPR signals at 3116 and 3305 G during the photolysis provide interesting information on the photochemical stability of the dinitrenes (Figure 2). The high intensity of the signal at 3116 G indicates a rather high photochemical stability of quintet dinitrene **9**, which is better protected by fluorine atoms from photochemical rearrangements into low-spin products. Much less photochemically stable is quintet dinitrene **8**, where both nitrene centers can easily insert into neighboring bonds to form azirines. The photochemical rearrangements of heteroaryl nitrenes has been studied in detail recently. [15,16]

Zero-Field Splitting Parameters of Nitrenes. As previous EPR studies have shown,[1,11−14] triplet pyridyl nitrenes show zfs values D around 1.0−1.2 cm^{-1} and E values close to zero. For quintet pyridyl-2,4-dinitrenes $|D| = 0.19-0.23$ cm^{-1} and $|E| = 0.035-0.042$ cm^{-1} are frequently observed, whereas for quintet pyridyl-2,6-dinitrenes $|D| = 0.19-0.22$ cm^{-1} and $|E| = 0.055-0.064$ cm^{-1} are typical values. The septet trinitrenes **1** and **2** show D values of 0.098−0.100 cm^{-1} and E values close to zero. Starting with these data, we simulated the EPR spectra of all five nitrenes (**6**, **7**, **8**, **9**, and **10**) formed during the photolysis of triazide **5** (Figure 2). The best fits were found for triplet nitrene **6** with $D = +1.041$ cm^{-1} and $E = 0$, for triplet nitrene **7** with $D = +1.143$ cm^{-1} and $E = 0$, for quintet dinitrene **8** with $D = +0.213$ cm^{-1} and $E = -0.0556$ cm^{-1}, for quintet dinitrene **9** with $D = +0.215$ cm^{-1} and $E = -0.0390$ cm^{-1}, and finally for septet trinitrene **10** with $D = -0.1018$ cm^{-1} and $E = +0.0037$ cm^{-1}.

The assignments of signs of D and E are based on the features of the tensor $\hat{\mathbf{D}}$ for triplet,[17] quintet,[14] and septet[2] nitrenes. The shape and resonance magnetic fields of all components in the EPR spectra did not change between 4 and 30 K. In the triplet nitrenes **6** and **7** the substituent effects of the two fluorine atoms (spin-repulsive) and the two azido groups (spin-accepting) almost cancel, and thus the zfs parameters of these nitrenes do not considerably differ from that of the unsubstituted triplet pyridyl-4-nitrene ($D = 1.107$ cm^{-1}, $E = 0$)[17] and pyridyl-2-nitrene ($D = 1.060$ cm^{-1}, $E = 0$).[18] These nitrenes show nearly degenerate $2p_x$ and $2p_y$ magnetic orbitals ($E = 0$), which indicates the lack of strong interactions between the $2p_y$ orbitals in the nitrene C−N bonds.[19] According to B3LYP/6-311+G** calculations the bond lengths in nitrenes **6** and **7** are about 1.33 Å.

The zfs parameters D and E of quintet dinitrene **9** are typical for quintet dinitrenes with angles between the two nitrene C−N bonds of 120−125°.[9,10] All dinitrenes of this type usually show very similar EPR spectra, characteristic of quintet spin states with $|E/D| \approx 1/5$. Indeed, DFT calculations predict the angle 2α between the two nitrene C−N bonds in **9** of 122.7°. The quintet ground spin state of dinitrene **9** follows from exchange interactions between the nitrene centers in positions 2 and 4 of the pyridine ring with spin densities of 1.6297 and 1.6667, respectively. Since the magnetic p-orbitals lying in the plane and perpendicular to the plane of dinitrene **9** have different projections on the axes X and Y (Scheme 3), these orbitals are magnetically nonequivalent, resulting in the large E value of **9**. An even larger E value is observed for quintet dinitrene **8** with an angle 2α between the two nitrene C−N bonds of 116.7°. The ground quintet spin state of this dinitrene is stabilized because of exchange interactions between the nitrene centers in positions 2 and 6 of the pyridine ring, showing spin densities of 1.7313 and 1.7370, respectively.

The EPR spectrum of dinitrene **8** is typical for quintet spin states with $|E/D| \approx 1/4$. A similar EPR spectrum has recently been described for quintet 4-amino-3,5-dichloropyridyl-2,6-dinitrene ($D = 0.210$ cm^{-1}, $E = -0.056$ cm^{-1})[14] matrix-isolated

(7) Chapyshev, S. V.; Walton, R.; Lahti, P. M. *Mendeleev Commun.* **2000**, *10*, 187–188.
(8) Chapyshev, S. V.; Kuhn, A.; Wong, M. W.; Wentrup, C. *J. Am. Chem. Soc.* **2000**, *122*, 1572–1579.
(9) Chapyshev, S. V.; Tomioka, H. *Bull. Chem. Soc. Jpn.* **2003**, *76*, 2075–2089.
(10) Chapyshev, S. V. *Russ. Chem. Bull.* **2006**, *55*, 1126–1131.
(11) Chapyshev, S. V.; Walton, R.; Lahti, P. M. *Mendeleev Commun.* **2000**, *10*, 114–115.
(12) Chapyshev, S. V.; Walton, R.; Serwinski, P. R.; Lahti, P. M. *J. Phys. Chem. A* **2004**, *108*, 6643–6649.
(13) Chapyshev, S. V.; Lahti, P. M. *J. Phys. Org. Chem.* **2006**, *19*, 637–641.
(14) Misochko, E. Ya.; Akimov, A. V.; Chapyshev, S. V. *J. Chem. Phys.* **2008**, *128*, Article No.124504.
(15) Bucher, G.; Siegler, F.; Wolff, J. J. *Chem. Commun.* **1999**, 2113–2114.
(16) Chapyshev, S. V. *Mendeleev Commun.* **2003**, *13*, 53–55.
(17) Wasserman, E. *Prog. Phys. Org. Chem.* **1971**, *8*, 319–336.
(18) Kuzaj, M.; Luerssen, H.; Wentrup, C. *Angew. Chem., Int. Ed. Engl.* **1986**, *25*, 480–482.
(19) Hebden, J. A.; McDowell, C. A. *J. Magn. Reson.* **1971**, *5*, 115–133.

in argon at 15 K. These results clearly demonstrate that the appearance of EPR spectra of quintet dinitrenes critically depends on the angle α, and even the small changes from 61.4° in **8** to 58.4° in **9** dramatically change the spectra. This is explained by changes in the orientations of the principal magnetic axes *Z*, *X*, and *Y* in the quintet dinitrenes when α decreases from 90° as in dinitrene **11**[20] to 0° as in dinitrene **12**[21] (Scheme 3). There are two critical points at α = 54.4° and 35.3° when |*E*/*D*| = 1/3.[14] Between these two critical points the axis *Y* transforms into the axis *Z* in order to keep |*E*/*D*| < 1/3. At α = 45 ° the *E* value should become equal to zero and the *D* value should reach its minimum. The closer α gets to 54.4°, the more sensitive the |*E*/*D*| ratio depends on the angle α.

EPR investigations on dinitrenes have primarily been carried out in organic glasses, so far. However, *D* and *E* values obtained in noble gas matrices can substantially differ from values obtained in organic glasses. Because of the lack of experimental data, these matrix effects have been neglected in the above discussion when comparing our data to literature values.

Assignments of Signals in EPR Spectra of Quintet and Septet Nitrenes. Complete assignments of all lines in powder EPR spectra of high-spin molecules with large *D* values have two fundamental problems. The first one is related with the presence of two terms in the spin Hamiltonian:

$$\mathbf{H} = g\beta\boldsymbol{HS} + \boldsymbol{SDS} \qquad (1)$$

containing different operators of the total electron spin angular momentum, $\hat{\boldsymbol{S}}_z$ and $\hat{\boldsymbol{S}}^2$. At high magnetic fields, when $g\beta\mathbf{H} \gg |D|$ and the Zeeman term $g\beta\boldsymbol{HS}$ dominates, the magnetic moment of the molecule processes around the field axis, and each of the transitions is characterized by a value of m_s, which is a "good" quantum number at this limit. At these high magnetic fields only the usual transitions $\Delta m_s = \pm 1$ are allowed. As the external magnetic field is lowered, the spin functions are mixed and m_s is no longer a "good" quantum number. Thus, at low magnetic fields the transitions $\Delta m_s = \pm 2$ become also allowed. However, some of the transitions $\Delta m_s = \pm 1$ and $\Delta m_s = \pm 2$ will not be observable if $(|D|+|3E|) > h\nu \cong 0.33$ cm^{-1}. The second problem consists in the appearance of additional "extra lines" in the powder EPR spectra from off-principal-axis oriented molecules, the principal magnetic axis *Z* of which forms the polar angle θ with the field axis. The number and field position of such "extra lines" can be different, depending on the zfs parameters and molecular symmetry. So far, only a few "extra lines" have unambiguously been identified in EPR spectra of quintet dinitrenes with $|E/D| \approx 0$[20] and 1/5.[22] The presence of strong $\Delta m_s = \pm 2$ transitions in powder EPR spectra of quintet dinitrenes with $|E/D| \approx 1/5$ has been discovered only recently.[10]

To perform a complete and unambiguous assignment of all lines in the EPR spectra of quintet dinitrenes **8**, **9** and septet trinitrene **10**, the Zeeman energy levels for the canonical orientations (**H**||**X**, **H**||**Y**, **H**||**Z**) of quintet and septet molecules and the angular dependencies of the resonance magnetic fields from the direction of the applied magnetic field were calculated (Figures 3−8). In strict accord with theory,[23] the exact numerical

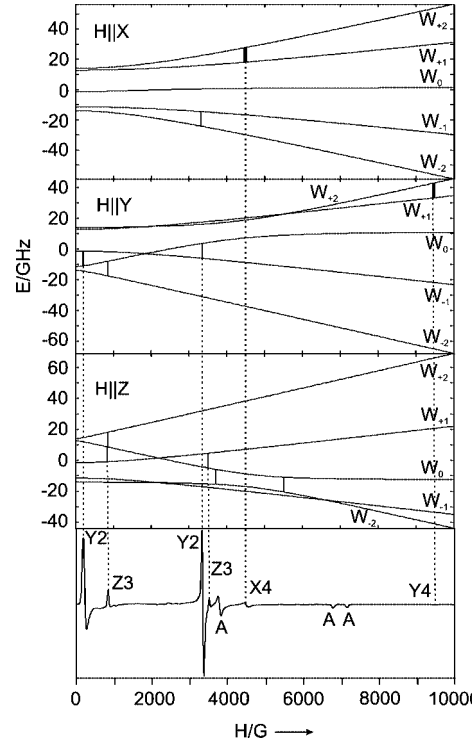

FIGURE 3. Zeeman levels and allowed $\Delta m_s = \pm 1$ transitions of quintet dinitrene **8**.

solution of the quintet spin-state Hamiltonian for dinitrene **8** with *S* = 2, *g* = 2.0023, *D* = +0.213 cm^{-1}, and *E* = −0.0556 cm^{-1} gives five zero-field energy levels: $W_1 = -2D(1+\alpha)^{1/2} = -14.02$ GHz, $W_2 = -D - 3E = -11.39$ GHz, $W_3 = -D + 3E = -1.39$ GHz, $W_4 = 2D = 12.77$ GHz, and $W_5 = 2D(1+\alpha)^{1/2} = 14.04$ GHz, where $\alpha = 3E^2/D^2$ (Figure 3). Due to the large *D* and *E* values only seven $\Delta m_s = \pm 1$ transitions of high probability can be observed in the spectrum at 203, 846, 3309, 3340, 3517, 4486 and 9465 G. These are two *X* (|−2 > ↔|−1 > and |+1 > ↔|+2 >), three *Y* (one |+1 > ↔|+2 > and two |−1 > ↔|0 > because of mixing of the spin functions at low and intermediate magnetic fields), and two *Z* (both|0 > ↔|+1 >) transitions. Three other lines at 3800, 6700,+ and 7100 G do not fit to any of the canonical transitions and should be assigned to "extra lines". These three lines are marked as **A** in Figure 3. The angular dependencies of the resonance magnetic fields (H_r) from the polar angle θ for dinitrene **8** are shown in Figure 4. Due to the magnetic nonequivalence of the molecular *X* and *Y* axes, the angular dependence of the resonance magnetic fields is different in the *ZY* ($\phi = \pi/2$, upper panel) and *ZX* planes ($\phi = 0$, lower panel). EPR peaks appear in the powder EPR spectra if $d\theta/dH_{res}$ is turned to infinity. All of the allowed transitions for the canonical orientations are well-resolved in the spectrum. Three additional "extra lines" are also clearly seen in Figure 4. The first one at 3800 G appears in the spectrum because the |0 > ↔|+1 > *Z* transition undergoes a singularity $d\theta/dH_r = \infty$ in the *ZX* plane at $\theta = 35°$. The other two "extra lines" are the result of singularities of the |0 > ↔|+1 > *Z* and |−1 > ↔|0 > *Y* transitions in the *ZY* plane at $\theta = 70°$ and 25°, respectively.

The Zeeman energy levels and angular dependencies of the resonance magnetic fields from the direction of the applied magnetic field calculated for dinitrene **9** with S = 2, *g* = 2.0023, *D* = +0.215 cm^{-1} and *E* = −0.0390 cm^{-1} are shown in Figures 5 and 6. Despite the larger *D* value, the energy gap between

(20) Kalgutkar, R. S.; Lahti, P. M. *Tetrahedron Lett.* **2003**, *44*, 2625–2628.
(21) Kalgutkar, R. S.; Lahti, P. M. *J. Am. Chem. Soc.* **1997**, *119*, 4771–4772.
(22) Fukuzawa, T. A.; Sato, K.; Ichimura, A. S.; Kinoshita, T.; Takui, T.; Itoh, K.; Lahti, P. M. *Mol. Cryst. Liq. Cryst.* **1996**, *278*, 253–258.
(23) Weltner, W., Jr. *Magnetic Atoms and Molecules*; Dover Publications: New York, 1989.

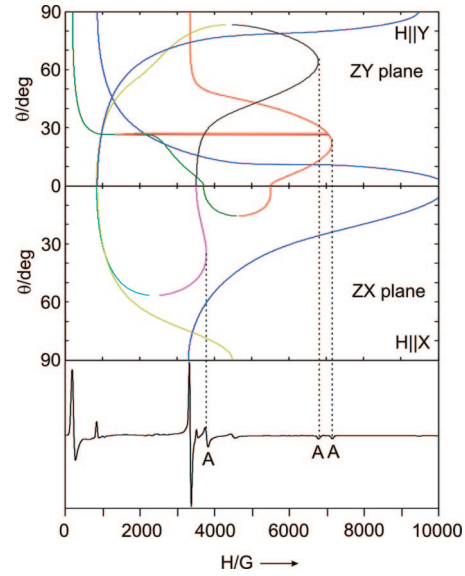

FIGURE 4. Dependence of transitions in EPR spectrum of quintet dinitrene **8** from the angle θ.

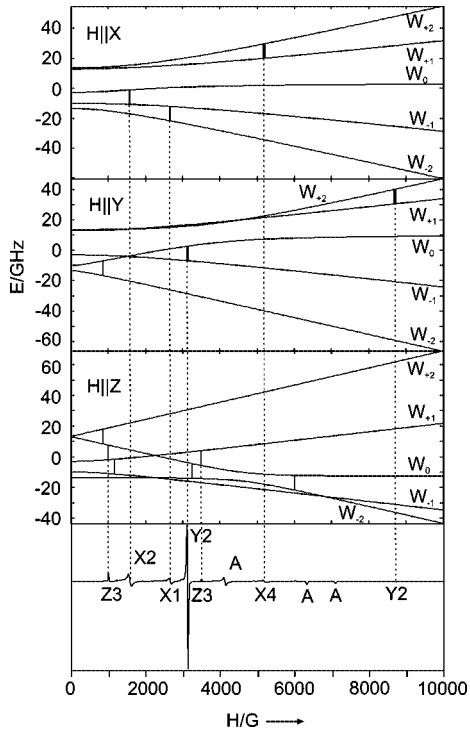

FIGURE 5. Zeeman levels and allowed $\Delta m_s = \pm 1$ transitions of quintet dinitrene **9**.

the levels W_1 and W_5 in this dinitrene is by 1.02 GHz smaller than in dinitrene **8**, caused by the higher E value of the latter. The five energy levels of dinitrene **9** at zero field have the following values: −13.51, −9.95, −2.94, 2.89, and 13.51 GHz. In contrast to dinitrene **8**, quintet dinitrene **9** has three X ($|-2> \leftrightarrow |-1>$, $|-1> \leftrightarrow |0>$, and $|+1> \leftrightarrow |+2>$), two Y ($|+1> \leftrightarrow |+2>$ and $|-1> \leftrightarrow |0>$), and two Z (both $|0> \leftrightarrow |+1>$) transitions of high probability. All of these transitions are well-resolved in the spectrum. The spectrum also contains three "extra lines" at 4200, 6300, and 7100 G that are the result of singularities of the $|-1> \leftrightarrow |0>$ Z transition in the ZX plane at $\theta = 40°$ and $|0> \leftrightarrow |+1>$ Z and $|-1> \leftrightarrow |0>$ Y transitions in the ZY plane at $\theta = 65°$ and 20°, respectively.

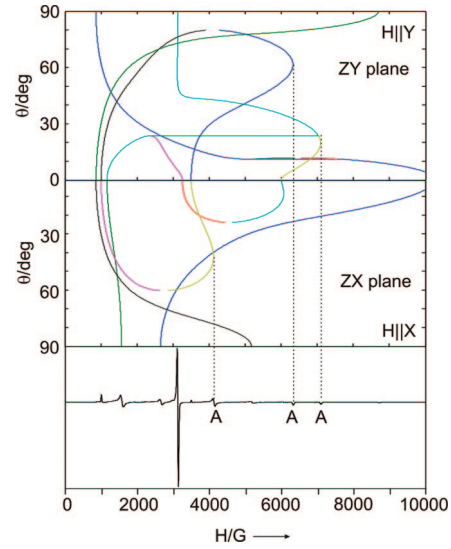

FIGURE 6. Dependence of transitions in EPR spectrum of quintet dinitrene **9** from the angle θ.

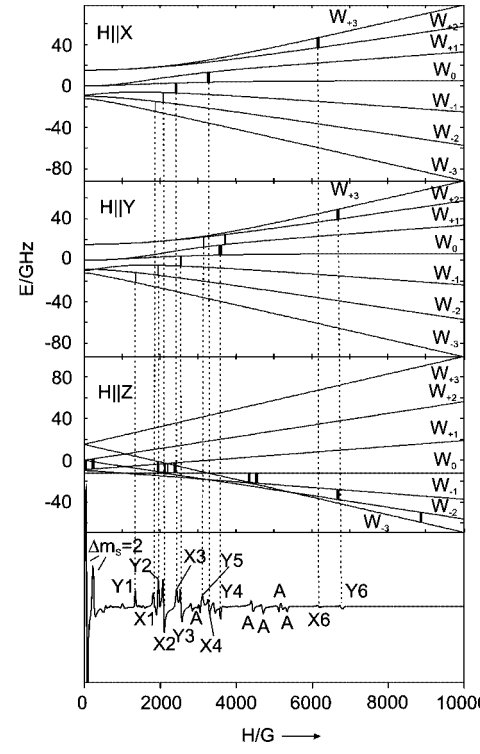

FIGURE 7. Zeeman levels and $\Delta m_s = \pm 1$ and ± 2 transitions of septet trinitrene **10**.

The Zeeman energy levels and angular dependencies of the resonance magnetic fields from the direction of the applied magnetic field calculated for trinitrene **10** with $S = 3$, $g = 2.0023$, $D = -0.1018$ cm^{-1}, and $E = +0.0037$ cm^{-1} are shown in Figures 7 and 8. Owing to the small value of E, the septet molecule has only five energy levels at zero field: $W_1 = -12.27$, $W_2 = -9.78$, $W_3 = -8.50$, $W_{4,5} = 0.06$, and $W_{6,7} = 15.27$ GHz with an energy gap between W_1 and W_5 of 27.54 GHz. This splitting is somewhat larger than the splitting between the outer levels in quintet dinitrene **9** and smaller than that in quintet dinitrene **8**. For the three canonical molecular orientations **H**||**X**, **H**||**Y** and **H**||**Z**, only five X but seven Y and ten Z transitions have high probability (Figure 7). However, a much smaller

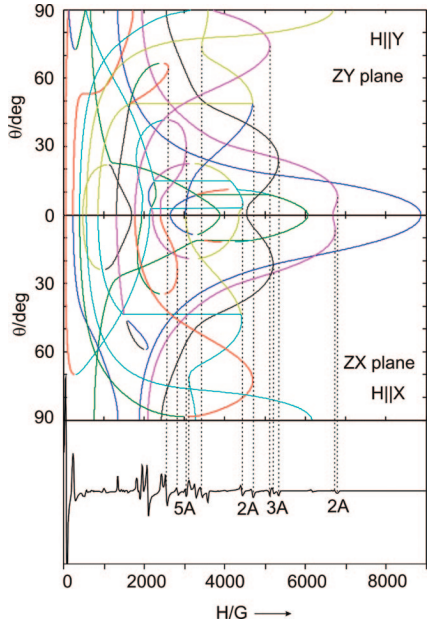

FIGURE 8. Dependence of transitions in EPR spectrum of septet trinitrene **10** from the angle θ.

number of transitions is observed in the experimental spectrum. These are the two very strong $\Delta m_s = \pm 2$ *Z* transitions at 90 and 248 G, five strong $\Delta m_s = \pm 1$ *X* transitions, and six also strong $\Delta m_s = \pm 1$ *Y* transitions. None of the six $\Delta m_s = \pm 1$ *Z* transitions can be detected in the experimental spectrum. As in the case of quintet dinitrenes **8** and **9**, the powder EPR spectrum of septet trinirene **10** contains "extra lines" from off-principal-axis oriented molecules (in total 13 signals, Figure 8). Six "extra lines" arise from the septet molecules that are rotated in the *ZX* plane with $\theta = 10°$, 25°, 50°, and 75°. Seven other "extra lines" arise from the septet molecules that are rotated in the *ZY* plane with $\theta = 8°$, 25°, 35°, 48°, 63°, 71°, and 74°. Two $\Delta m_s = \pm 2$ *Z* transitions at 90 and 248 G have very high intensities because this type of transitions is almost independent of molecular orientations. Thus, for instant, the strongest line at 90 G is produced by a large number of molecules that have $\theta = 0-70°$ orientation in both the *ZX* and *ZY* planes.

In septet trinitrene **10** three triplet centers are involved in strong ferromagnetic exchange interactions that resemble molecular domains in magnetic materials. According to theory,[2] the principal magnetic axes for such molecules are oriented as shown in Scheme 4. The rather large *E* value of septet trinitrene **10** indicates that its magnetic axes *X* and *Y* are not equivalent. Most likely this is caused by the strong conjugation of the γ-nitrene unit with the pyridine ring, changing the spatial orientations of the magnetic orbitals in this unit. Indeed, the UB3LYP/6-311+G** calculations predict very different spin densities and C−N bond lengths for the α- and γ-nitrene units, respectively, of septet **10** (for α-nitrene units $\rho_N = 1.7266$, $r_{CN} = 1.3344$ Å, whereas for γ-nitrene units $\rho_N = 1.6503$, $r_{CN} = 1.3180$ Å). Due to the strong conjugation with the pyridine ring, the γ-nitrene center exhibits a very short C−N bond and rather low spin density at the nitrogen atom. In contrast, the α-nitrene centers of septet **10** show relatively high spin densities at the nitrogen atoms and comparatively long C−N distances.

All of these effects can schematically be described with the resonance structures **10a** and **10b** (Scheme 4). The resonance form **10b** illustrates that the γ-nitrene unit of septet **10** has properties of an sp^2 center, resulting in different projections of the local tensor D_{xx} on the molecular axes X and Y. The noticeable contribution of the quinonoid form **10b** in the electronic structure of septet trinitrene **10** as well as very high spin densities on the α-nitrene units of this trinitrene are probably those factors that decrease its kinetic stability. The isolation of this highly reactive intermediate requires matrix isolation in inert gases, whereas the isolation in frozen organic solutions is impossible. This is in line with previous studies that have shown that triplet arylnitrenes with very high spin densities at the nitrene centers readily insert into C−H bonds of hydrocarbons similar to singlet nitrenes.[24]

Conclusions

Matrix isolation in argon at 4 K provides a way to generate and spectroscopically characterize highly reactive trinitrenes even in cases were low-temperature organic glasses fail to stabilize these elusive molecules. Using this technique, septet 3,5-difluoropyridyl-2,4,6-trinitrene **10** along with quintet 2-azido-3,5-difluoropyridyl-4,6-dinitrene **8**, quintet 4-azido-3,5-difluoropyridyl-2,6-dinitrene **9**, triplet 2,6-diazido-3,5-difluoropyridyl-4-nitrene **7**, and triplet 2,4-diazido-3,5-difluoropyridyl-6-nitrene **6** have been obtained by the photolysis of 2,4,6-triazido-3,5-difluoropyridine **5**. High-resolution EPR spectra of all high-spin nitrenes were obtained, from which the zfs parameters could be determined with high accuracy. By analyzing the signal intensities we conclude that the two isomeric mononitrenes **6** and **7** are formed simultaneously. Unlike with other triazides, the photolysis of **5** does not lead to the preferential cleavage of one of the azide groups. The same is true for the subsequent loss of the second nitrogen molecule, which leads to a mixture of the isomeric quintet dinitrenes **8** and **9** with no obvious preference. The septet trinitrene **10** is the final photoproduct and is very stable in argon matrices toward further irradiation. The formation of low-spin products upon prolonged irradiation with light at $\lambda > 305$ nm was not observed in our experiments.

The EPR spectrum recorded for dinitrene **8** represents a new type of spectrum that is characteristic for quintet molecules with $|E/D| \approx 1/4$ and dipolar angles $2\alpha \approx 117°$ between two ferromagnetically interacting triplet sites. The EPR spectrum of dinitrene **9** with $2\alpha \approx 122.2°$ is identical to spectra of many other quintet dinitrenes with $|E/D| \approx 1/5$. Quintet dinitrene **8** with $D = +0.213$ cm^{-1} and $E = -0.0556$ cm^{-1} displays in the spectrum two *Z*, three *Y*, and one *X* $\Delta m_s = \pm 1$ transitions, and in addition three "extra lines" from off-principal-axis oriented molecules. Quintet dinitrene **9** with $D = +0.215$ cm^{-1} and $E = -0.0390$ cm^{-1} shows in the spectrum two *Z*, three *Y*, and three *X* $\Delta m_s = \pm 1$ transitions plus also three "extra lines" from off-principal-axis oriented molecules. Septet trinitrene **10** with $D = -0.1018$ cm^{-1} and $E = +0.0037$ cm^{-1} displays in the spectrum two strong $\Delta m_s = \pm 2$ *Z* transitions in magnetic fields below 900 G, no *Z*, six *Y*, and five *X* $\Delta m_s = \pm 1$ transitions plus 13 "extra lines" from off-principal-axis oriented molecules. Thus, the high resolution of the EPR spectra in solid argon allows a complete assignment of the experimentally observed transitions in the nitrenes with triplet, quintet, and septet ground states. All lines in the powder EPR spectrum of the septet trinitrene were, for the first time, unambiguously assigned on the basis of eigenfield calculations of the Zeeman energy levels and angular dependencies of the resonance fields. Both EPR

(24) Kayama, R.; Shizuka, H.; Sekiguchi, S.; Matsui, K. *Bull. Chem. Soc. Jpn.* **1975**, *48*, 3309–3312.

SCHEME 4. Principal Magnetic Axes and Resonance Structures for Septet Trinitrene 10

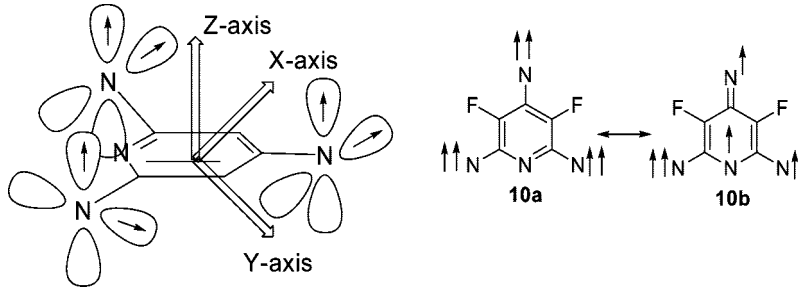

studies and DFT calculations indicate that the septet trinitrene has two different types of nitrene units. One of them in position 4 of the pyridine ring has a short C−N bond and low spin density at the nitrogen atom. Its local tensor D_{xx} gives different projections on the molecular *X* and *Y* axes, which results in a rather large *E* value of the septet molecule. By contrast, the α-nitrene units of **10** have slightly elongated C−N bonds and very high spin densities at the nitrogen atoms. These nitrene units are responsible for the rather large *D* value of septet trinitrene **10** and its very high reactivity in frozen organic solutions.

Experimental Section

Triazide **5** was synthesized by the reaction of pentafluoropyridine with NaN_3 according to the literature procedure.[25]

X-band EPR spectra were recorded with a Bruker Elexsys E500 EPR spectrometer with an ER077R magnet (75 mm gap between pole faces), an ER047 XG-T microwave bridge, and an ER4102ST resonator with a TE_{102} cavity. The matrices were deposited on an oxygen-free high-conductivity copper rod (75 mm length, 3 mm diameter) cooled by a Sumitomo SHI-4-5 closed-cycle 4.2 K cryostat.

The vacuum system consisted of a vacuum shroud equipped with a sample inlet valve and a half-closed quartz tube (75 mm length, 10 mm diameter) at the bottom and a vacuum pump system with a turbo molecular pump backed by a two-stage, rotary-vane pump. To avoid contamination of the high-vacuum segment by pump oil from the backing pump, a catalytic oxidation filter was placed between the rotary-vane pump and the turbo pump. During deposition, the inlet port was positioned at the same height as the tip of the copper rod. For irradiation, the copper rod was lowered into the quartz tube at the bottom of the shroud, and for the measurement of the EPR spectra, the whole apparatus was moved downward so that the quartz tube and copper rod were positioned inside the EPR cavity.

Triazide **5** was evaporated at 25 °C and co-deposited with a large excess of argon (99.9999%) on the tip of the copper rod at 4 K. The matrix-isolated sample was irradiated with a high-pressure mercury lamp, using a filter passing the light at $\lambda > 305$ nm, and spectra were recorded at various irradiation times.

The computer simulations of EPR spectra were performed by using the XSophe computer simulation software suite (version 1.0.4)[26] and by using the EasySpin program package (version 2.6.1).[27] The simulations were performed by using a matrix diagonalization methods for $S = 1$, 2, or 3 using the parameters $\nu = 9.5946$ GHz, $g = 2.0023$ and line widths $\Delta H = 40$ G for $S = 1$ and 30 G for $S = 2$ and 3, respectively. The parameters *D* and *E* obtained from the simulations fitted the experimental spectra within ± 0.0003 and ± 0.0001 cm^{-1}, respectively. The EasySpin program package was used for the eigenfield calculations of the Zeeman energy levels for canonical orientations of the tensor $\hat{\mathbf{D}}$ (**H**||**X**, **H**||**Y**, **H**||**Z**) and for calculating the angular dependencies of the resonance fields on rotating the tensor $\hat{\mathbf{D}}$ by the angle θ in two planes ($\phi = 0$ and $\phi = \pi/2$, where θ and ϕ are the Euler angles).

All density functional theory (DFT) calculations were performed with the Gaussian 98 program package.[28] The geometries of the molecules were optimized by using the B3LYP method[29] in combination with the 6-311+G** basis set. The nature of the stationary points was assessed by means of vibrational frequency analysis.

Acknowledgment. This work was financially supported by the Deutsche Forschungsgemeinschaft and the Fonds der Chemischen Industrie (W.S.). S.V.C. is grateful to the Russian Foundation for Basic Research (grant RFBR 05-03-32410) for financial support.

Supporting Information Available: Tables with *Z*-matrices and details of structure and spin density distribution of the nitrenes **6**−**10**. This material is available free of charge via the Internet at http://pubs.acs.org.

JO800425K

(25) Chapyshev, S. V. *Chem. Heterocycl. Compd.* **2001**, *37*, 968–975.

(26) Griffin, M.; Muys, A.; Noble, C.; Wang, D.; Eldershaw, C.; Gates, U. E.; Burrage, K.; Hanson, G. R. *Mol. Phys. Rep.* **1999**, *26*, 60–84.

(27) Stoll, S.; Schweiger, A. *J. Magn. Reson.* **2006**, *178*, 42–55.

(28) Ffisch, M. J.; Trucks, G. W.; Schlegel, H. B.; Scuseria, G. E.; Robb, M. A.; Cheeseman J. R.; Zakrzewski, V. G.; Montgomery, J. A., Jr.; Stratmann, R. E.; Burant, J. C.; Dapprich, S.; Millam, J. M.; Daniels, A. D.; Kudin, K. N.; Stain, M. C.; Farkas, O.; Tomasi, J.; Barone, V.; Cossi, M.; Cammi, R.; Mennucci, B.; Pomelli, C.; Adamo, C.; Clifford, S.; Ochterski, J.; Petersson, G. A.; Ayala, P. Y.; Cui, Q.; Morokuma, K.; Malick, D. K.; Rabuck, A. D.; Raghavachari, K.; Foresman, J. B.; Cioslowski, J.; Ortiz, J. V.; Baboul, A. G.; Stefanov, B. B.; Liu, G.; Liashenko, A.; Piskorz, P.; Komaromi, I.; Gomperts, R.; Martin, R. L.; Fox, D. J.; Keith, T.; Al-Laham, M. A.; Peng, C. Y.; Nanayakkara, A.; Gonazalez, C.; Challacombe, M.; Gill, P. M. W.; Johnson, B.; Chen, W.; Wong, M. W.; Andres, J. L.; Gonazalez, C.; Head-Gordon, M.; Replogle, E. S.; Pople, J. A. Gaussian 98, Revision A.9; Gaussian, Inc.: Pittsburgh, PA, 1998.

(29) Becke, A. D. *J. Chem. Phys.* **1993**, *98*, 5648–5652.